A Design Method for SLM-Parts Using Internal Structures in an Extended Design Space

Rene Bastian Lippert(✉) and Roland Lachmayer

Institute of Product Development,
Leibniz Universität Hannover, Hannover, Germany
lippert@ipeg.uni-hannover.de

Abstract. Selective laser melting enables the production of cavities as well as internal structures and thus opens up new lightweight potentials for mechanically loaded components. This paper describes a design method for weight-optimization by applying internal structures in an extended design space compared to conventional models. Based on a pedal crank as a demonstrator, the objective is a maximum weight reduction with predefined stresses and a homogeneous stress distribution. The basic dimensioning of the design space is limited by assembly and application restrictions. By using computer aided design tools and topology optimization in an iterative procedure, a step wise confinement of the design space takes place. Concerning the same interfaces and functions as the conventional pedal crank, new model generations with the advantage of force flow adapted structures are built up. Using Finite Element Method, a continuous evaluation of the impact from a change of design towards the weight/stress ratio is performed. The created models are evaluated regarding their weight reduction in order to select the most efficient one. The final model has a large-volume geometry with the simultaneous integration of internal structures and cavities. A validation compared to the initial model as well as to a model with conventional design space and selective areas with internal structures quantifies the optimization result. Based on the acquired knowledge from this comparison, an estimation of the weight reduction potential concerning the design method is given.

1 Introduction

Additive Manufacturing is used for the production of prototypes and tools. Also direct manufacturing, and thus the additive fabrication of end products to use or assemble directly, becomes increasingly more important [1, 2]. Due to the mechanical properties of the final components, especially selective laser melting serves as a continuous substitute as well as a supplement to conventional manufacturing processes [3, 4].

A major benefit in designing structural components using selective laser melting is the potential of light weight constructions [5, 6]. Here, the layer-wise and selective solidification permits new lightweight designs, such as manufacturing freeform geometries, undercuts or cavities [7–9]. To enlarge the weight-saving potential, internal structures can be implemented. These are defined as “repeatable elements for the substitution of solid volumes with the objective to vary the material arrangement on a

M. Meboldt and C. Klahn (eds.), *Industrializing Additive Manufacturing - Proceedings of Additive Manufacturing in Products and Applications - AMPA2017*,
DOI 10.1007/978-3-319-66866-6_2

macroscopic level without affecting the material properties" [10]. The challenge is the integration of load optimized internal structures in order to reduce the component weight without a significant increase of stresses, so that the life expectancy is not influenced [11, 12]. Here, computer-aided tools can be used to predict the component failure and to provide a force flow adapted orientation of internal structures [13, 14]. Previous studies have shown that the weight of a component can be reduced by around 30% using internal structures in conventional shapes [15, 16]. Based on these investigations, the present paper describes an analysis to increase weight saving by moving away from the conventional shapes and utilizing an extended design space.

2 Design Method

A computer-aided design method to implement internal structures in mechanically loaded components is described. It is distinguished into five sequentially arranged sections, which are characterized by an iterative procedure, shown in Fig. 1.

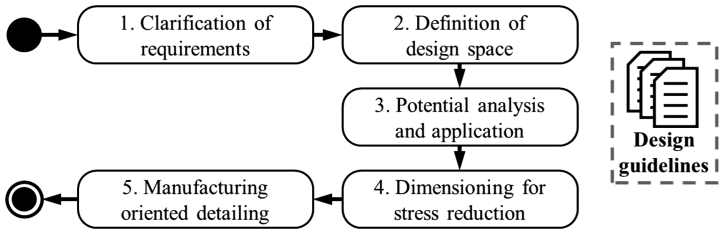

Fig. 1. Integrated design method using computer-aided modeling and simulation tools

To clarify the requirements (1), information about force application points, amount of load vectors as well as the stress state of the component has to be figured out. This information can be calculated or recirculated from life cycle data. Furthermore, a design space (2) has to be defined, which is limited by effective areas as well as assembly and application restrictions. Based on information about the mechanical behavior of internal structures and requirements of the component, suitable structures have to be selected and transferred into the design space (3) selectively. The structures and transition areas are optimized regarding stress reduction and a homogeneous stress distribution (4). The new model generation is finally validated regarding manufacturability (5) by considering design guidelines for detailing.

2.1 Design Guidelines for Internal Structures

To fulfill requirements of the manufacturing process in the early development stages, design guidelines have to be considered [17, 18]. In form of knowledge storages, such as checklists or design catalogues, these guideline provides standard values to ensure manufacturability [19]. For example, boundary conditions for minimal wall thickness or diameter, depending on the building direction of a component, are defined [20, 21].

Design guidelines are partially available for different parameter sets, which describe a specific machine and material. Furthermore, general statements are available, which define optimal orientation, arrangement or positioning of components in the process chamber or the necessity for cleaning openings [18]. As shown in Fig. 2, using the example of a honeycomb, minimum wall thicknesses, realizable overhangs and 45° angles to avoid support structures have to be considered. Furthermore, the element size b is limited by a minimal diameter.

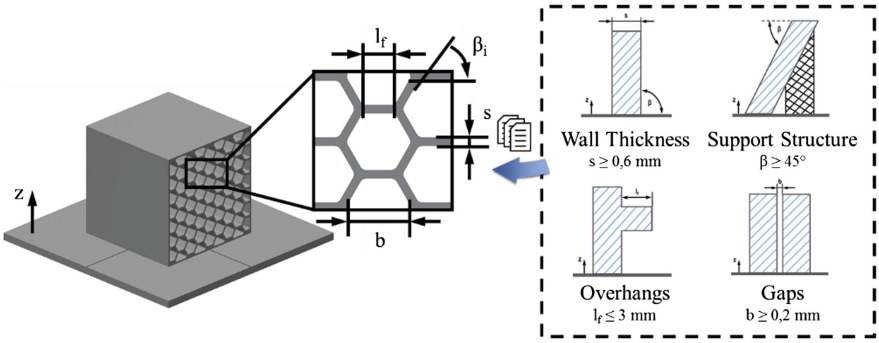

Fig. 2. Relevant design guidelines concerning the example of honeycomb structures

2.2 Simulation Environment

A material database to specify the anisotropic behavior of a selective laser melting component is defined. Using this database during computer-aided modeling and simulation, the consideration of building directions is possible. Analogous to conventionally processed materials, powder alloys for selective laser melting differ in mechanical properties depending on the post-process. Thus, the properties after the building process and a post-heat treatment are different. In practice, selective laser melting components are predominantly used after heat treatment, because internal stresses are reduced and the material properties are homogenized. Based on the example of AlSi10Mg alloy - which is used in this paper for validation - material characteristics after heat treatment (300 °C for 2 h) are shown in Fig. 3 [22, 23]. Besides the static properties, the stress-cycle (S-N) curve for calculating the fatigue properties is set [15].

	x-/y- direction	z-direction
E-Modul [kN/mm²]	70	60
Density [g/cm³]	2,67	2,67
Poisson's ratio	0,3	0,3
Tensile strength [kN/mm²]	345	350
Yield strength [kN/mm²]	245	245
Elongation at fracture [%]	12	11
Shear modulus [kN/mm²]	2,436 (yz/ xz)	2,6315 (xy)

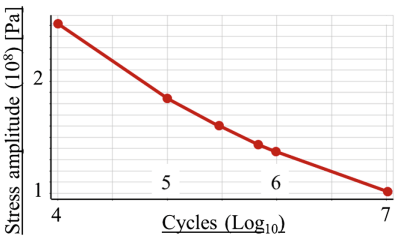

Fig. 3. Properties and S-N curve for AlSi10Mg after heat treatment [24–28]

3 Adaption of a Demonstrator

To validate the design method, a pedal crank is used as a demonstrator. The objective is a maximal weight reduction with constant internal (von Mises) stresses compared to conventional models (respectively material characteristics). Except considering relevant interfaces, the component dimensions are freely selectable.

3.1 Clarification of Requirements

The initial model is conventionally manufactured with AlSi10Mg alloy and has a weight of m = 217.45 g. Two interfaces for fixing the bottom bracket and the pedals define the length l = 170 mm, as depicted in Fig. 4-a. According to Sullivan und Chris, different load cases occur during the lifecycle. In assumption of an idealized model, in which torsional forces are neglected (due to the external force introduction), the critical load case is pure bending [16, 29]. In combination with the load vector F_{max} = 2.250 N, which represents the maximum occurring forces with an additional safety factor, the bending load is used for further optimization [29].

3.2 Definition of Design Space

As shown in Fig. 4-b, the design space is limited by assembly and application restrictions as well as the size of the process chamber (machine Eosint M280). This rough estimation is used as an input for topology optimization (using material characteristics shown in Fig. 3) in order to narrow down the design space. Figure 4-c shows the optimization results as an iterative elimination of the volume elements with the lowest stresses (Ansys Workbench 17.0). It can be seen that an asymmetric topology occurs. For the following potential analysis and selection of an internal structure, the optimization result is rebuilt as shown in Fig. 4-d.

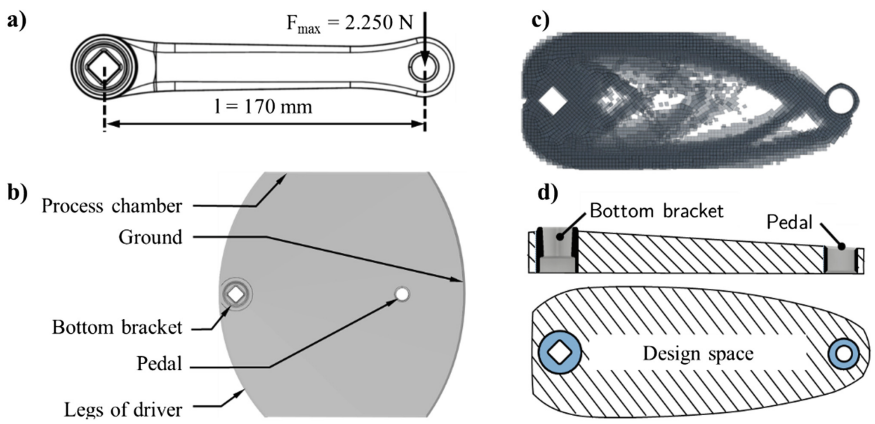

Fig. 4. Definition of design space (a) Relevant load case of the initial model (b) Assembly and application restrictions (c) Result of topology optimization (d) Extended design space

In order to identify a suitable internal structure to be integrated in the design space, the asymmetrical shape is neglected in the first iteration. The results are considered again while dimensioning for stress reduction. Hence, the topology is iteratively adapted to the asymmetric shape.

3.3 Potential Analysis and Application

Preliminary investigations at the institute describe the modeling and simulation of digital specimens with internal structures [9]. In addition to the application of computer-aided tools, the results are validated by analyzing physical specimens with a static test bench. The acquired knowledge is summarized in a design catalog, which allows the selection of a load optimized structure, when the load case is predefined. The essential criterion to select a suitable structure is low weight with high stiffness. Based on the findings summarized in the design catalog, suitable structures for bending loads are selected. Using CAD, these structures are modeled within the design space (e.g. see Fig. 5 - right) as separate concept models and are simulated by applying a structural mechanical analysis. The results are shown in Fig. 5 as a relation between (von Mises) stress and weight. Local stress peaks occurring on non-optimized transition regions (structure is unfavorably cut) are neglected. Furthermore, the stress/weight ratio of the initial model, the allowable stress σ_{all} of AlSi10Mg as well as an objective area are depicted.

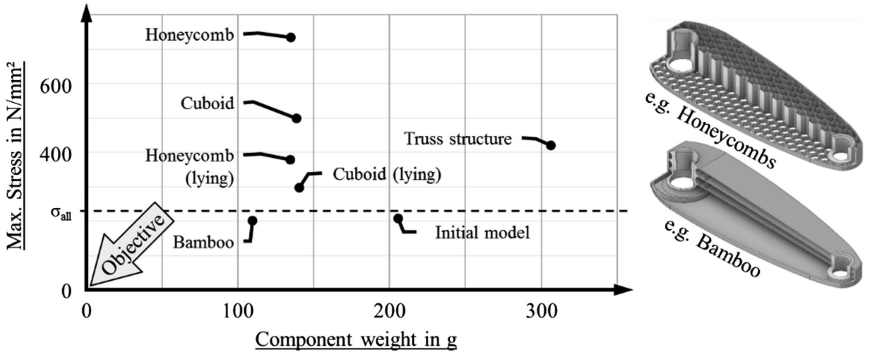

Fig. 5. Stress/weight ratio for concept models with different internal structures in the extended design space

Due to the high material effort, the concept model 'truss structure' (1) shows a higher component weight compared to the initial model. 'Honeycombs' and 'cuboids' show improved weight savings. However, the stresses partly increase significantly ($\sigma_{max} >> \sigma_{allowable}$).

The concept model 'bamboo' already shows a synthesis between maximum stresses and component weight and thus is selected for the further optimization.

3.4 Dimensioning for Stress Reduction

To define a preliminary design, the topology of the concept model 'bamboo' undergoes a rough adaption to the asymmetrical shape originating from the topology optimization (see Fig. 6-a). It can be seen that high stresses occur in the area of the bearing ($\sigma \approx 280$ N/mm^2), which exceed the allowable value $\sigma_{allowable} \approx 245$ N/mm^2. Furthermore, low stresses occur along the neutral axis.

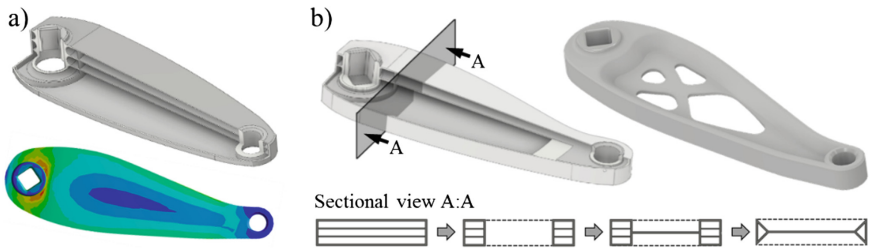

Fig. 6. Optimizing the topology for stress reduction (a) Adapting the outer shape (b) Adapting the cross-sectional area

In a first step, the areas with low stresses are optimized by removing material according to the optimization results (see Fig. 6-b). Starting from the concept model with a constant cross-sectional area (A:A), various preliminary designs are examined. As a result, a hollow profile with 45°-surfaces is provided in the outer areas. The less stressed area is substituted by a thin layer without cavities. Due to this modification, material can be saved and manufacturability can be improved by reducing overhangs.

After adapting both, the outer shape and the cross-section area, the stress distribution of the preliminary design can be improved, as depicted in Fig. 7-a. However, the maximum stress is still critical. Against this background, the areas near the bearing has to be optimized. After evaluating different strategies for the material distribution, an adapted "core" is built up, shown in Fig. 7-b. Holes are used for maximum weight reduction. The optimization of the preliminary design results in a homogeneous stress distribution with maximum stresses ($\sigma \approx 240$ N/mm^2) below the allowable values.

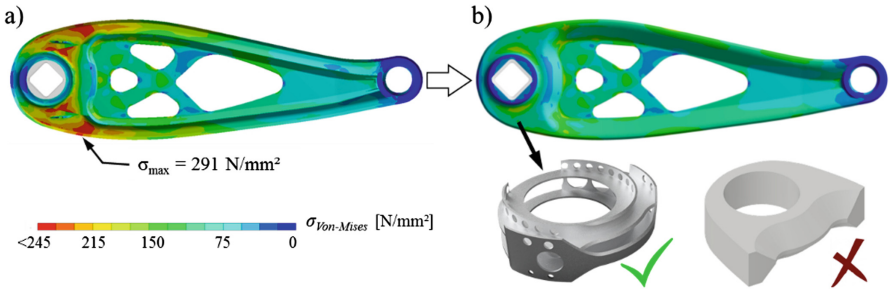

Fig. 7. Stress distribution while dimensioning (a) Adapted cross-sectional area (b) Stress-optimized model

3.5 Manufacturing Oriented Detailing

The preliminary design is finally evaluated in comparison to the design guidelines. Therefore, the orientation and position of the model in the process chamber has to be defined. After weighing the criteria for production time, accuracy, loading capacity due to anisotropy, post-process effort and avoiding damage by the coater, the orientation and position is set as depicted in Fig. 8.

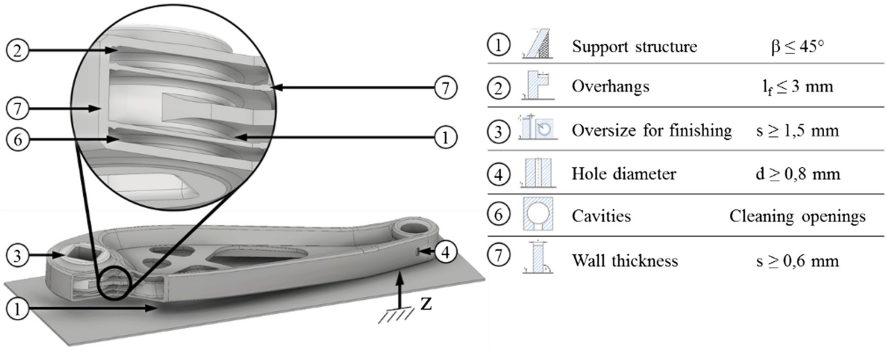

Fig. 8. Relevant design guidelines for the optimized model of the pedal crank

Due to the horizontal positioning various areas result, which are limited by design guidelines. For example, down skin surfaces - normal vector is negative in respect to z direction - have to be investigated with regards to necessity of support structures. Supports are unavoidable between the component and building platform, but can be easily removed in post-process. In the components' interior, supports are forbidden, because removing them is impossible. Consequently, cavities as well as internal structures are limited by maximum overhangs and angles. Considering this restriction, all down-skin surfaces can be manufactured without lowering in negative z direction during manufacturing.

Besides specific values, general guidelines for removing excess material have to be considered. As depicted in Fig. 8, cleaning openings are provided on a slightly loaded area of the surface. The sizing of the openings is limited by the minimum diameter in z direction. Furthermore, the consideration of minimizing stress peaks and avoiding supporting structures is necessary during designing.

4 Conclusion

The optimized model is manufactured with AlSi10Mg using an Eosint M280 machine. As depicted in Fig. 9-a, the process parameters for core and skin exposure are set. Figure 9-b shows the result from manufacturing process after thermal (300 °C for 2 h) and mechanical post-processing (removing support structures and shot peening). The outer shape shows a high accuracy corresponding to the CAD model. To evaluate the

accuracy of the internal structure, a mechanically sliced model is shown in addition. The estimation shows, that an accurate realization of the inner structures without deformation took place.

	Power in W	Speed in mm/s
Core	370	1.300
Up-/ Downskin	370	775
Postcontours	370	230

Fig. 9. Process parameters (Eos EoSint M280) and results from manufacturing process

Internal surfaces with a down-skin angle $\beta > 45°$ have a good surface quality. As expected, overhangs show an increased surface roughness. Compared to the weight of the initial model ($m \approx 217$ g), a weight saving of about 55% is achieved. Due to its complexity, the new optimized model ($m \approx 88$ g) cannot be manufactured using conventional technologies. In comparison to previous investigations, in which the shape of the initial model is maintained, further weight savings are achieved. The maximum (von Mises) stresses increased marginally, but are located below the allowable value $\sigma_{allowable}$.

A high optimization effort is necessary to achieve the obtained results. A rough transfer of a structure as a concept model can be performed in a first iteration without great effort. However, the stress- and manufacturing-oriented detailing of the preliminary design increase this effort significantly.

In addition to influences during modeling and simulation, internal structures have an effect on the in- and post-process. On one hand, the manufacturing time is affected. On the other hand, the post-process is challenging. This concerns the quality control of internal surfaces for comparison with the CAD geometry. Furthermore, internal structures hinder conventional mechanical finishing, which is necessary to improve mechanical behavior.

In the next step, the fatigue performance has to be simulated in order to calculate life expectancy. In addition, physical models have to be analyzed by performing static and fatigue tests. The acquired results are compared with the digital models. The objective is to describe design guidelines for covering surface roughness and mechanical properties in form of safety values during the design phase.

The challenge to implement the integrated design method is reproducibility and automation. Stress- and manufacturing-oriented detailing is strongly component specific and can only be generalized with difficulty. First approaches describe the parameterized density variation based on the amount of internal stresses.

References

1. Gibson, I., Rosen, D., Stucker, B.: Additive Manufacturing Technologies: 3D Printing, Rapid Prototyping, and Direct Digital Manufacturing. Springer (2015). ISBN 978-1-4939-2112-6
2. Gartner Marktforschungsunternehmen: Hype cycle for emerging technologies maps the journey to digital business (2014). www.gartner.com. Accessed 17 June 2016
3. Gebhardt, A.: Generative Fertigungsverfahren: Additive Manufacturing und 3D Drucken für Prototyping – Tooling – Produktion, 4th edn. Hanser (2013)
4. Poprawe, R., et al.: Production systems: recent developments in process development, machine concepts and component design. In: Advances in production Technology. Springer (2015)
5. Emmelmann, C., Sander, P., Kranz, J., Wycisk, E.: Laser additive manufacturing and bionics: redefining lightweight design. Phys. Proc. **12**, 364–368 (2011)
6. Teufelhart, S.: Geometrie- und belastungsgerechte Optimierung von Leichtbaustrukturen für die additive Fertigung. Additive Fertigung, Seminarbericht (2012)
7. Lippert, R.B., Lachmayer, R.: Topology examination for additive manufactured aluminum components. In: Proceedings of the 3rd DDMC, Berlin, Germany (2016)
8. Hague, R., Mansour, S., Saleg, N.: Design opportunities with rapid manufacturing. Assem. Autom. **23**(4), 346–356 (2002)
9. Chen, T., Fritz, S., Shea, K.: Design for mass customization using additive manufacturing: case-study of a balloon-powered car. In: Proceedings of the 20th ICED15, Milan, Italy (2015)
10. Lippert, R.B., Lachmayer, R.: Bionic inspired infill structures for a light-weight design by using SLM. In: Proceedings of the 14th DESIGN Conference, Dubrovnik, Croatia (2016)
11. Smith, M., et al.: Finite element modelling of the compressive response of lattice structures manufactured using the selective laser melting technique. Int. J. Mech. Sci. **67**, 28–41 (2013)
12. Lachmayer, R., Lippert, R.B., Fahlbusch, T.: 3D-Druck beleuchtet – Additive Manufacturing auf dem Weg in die Anwendung. Springer, Germany (2016). ISBN 978-3-662-49055-6
13. Ullah, I., et al.: Performance of bio-inspired kagome truss core structures under compression and shear loading. J. Compos. Struct. **118**, 294–302 (2014)
14. Reinhart, G., Teufelhart, S.: Load-adapted design of generative manufactured lattice structures. Phys. Proc. **12**, 385–392 (2011)
15. Lippert, R.B., Lachmayer, R.: Einflussfaktoren innerer strukturen im gestaltungsprozess von strukturbauteilen für das selektive laserstrahlschmelzen. In: Proceedings of the 14th Rapid. Tech, Erfurt, Germany (2017)
16. Lachmayer, R., Lippert, R.B.: Additive Manufacturing Quantifiziert. Springer, Heidelberg, May 2017. ISBN 978-3-662-54112-8
17. Vayre, B., et al.: Designing for additive manufacturing. In: 45th CIRP Conference on Manufacturing Systems (2012)
18. VDI 3405 Part 3: Additive manufacturing processes, rapid manufacturing - design rules for part production using laser sintering and laser beam melting. Beuth, Berlin, Germany (2015)

19. Roth, K.: Konstruieren mit Konstruktionskatalogen - Band 1: Konstruktionslehre, 3. Auflage. Springer, Germany (2000). ISBN 978-3-642-17466-7
20. Zimmer, D., Adam, G.: Direct manufacturing design rules. In: Innovative Developments in Virtual and Physical Prototyping (2012)
21. Kranz, J., Herzog, D., Emmelmann, C.: Design guidelines for laser additive manufacturing of lightweight structures in TiAl6V4. J. Laser Appl. **27**, S14001 (2015)
22. EOS GmbH: Material data sheet EOS Aluminium AlSi10Mg. EOS GmbH (2014)
23. DIN EN 515:2016-01: Aluminium und Aluminiumlegierungen - Halbzeug - Bezeichnungen der Werkstoffzustände. Beuth Verlag (2015)
24. Tang, M., Pistorius, P.C.: Oxides, porosity and fatigue performance of AlSi10Mg parts produced by selective laser melting. Int. J. Fatigue **94**, 192–201 (2016)
25. Brandl, E., Heckenberger, U., Holzinger, V., Buchbinder, D.: Additive manufactured AlSi10Mg samples using Selective Laser Melting (SLM): microstructure, high cycle fatigue, and fracture behavior. Mater. Des. **34**, 159–169 (2012)
26. Kempen, K., Thijs, L., Van Humbeeck, J., Kruth, J.P.: Mechanical properties of AlSi10Mg produced by selective laser melting. Phys. Proc. **39**, 439–446 (2012). doi:10.1016/j.phpro.2012.10.059
27. Anyalebechi, P.: Effect of process route on the structure, tensile, fatigue properties of aluminum alloy steering knuckles. Int. Foundry Res. **63**(3), 32–43 (2011)
28. Humbeeck, J.V., Thijs, L.: PFC: AlSi10Mg parts produced by Selective Laser Melting (SLM). Miguel Godino Martínez. Industrial Engineering. Specialty: Materials (2013)
29. Sullivan, S., Chris, H.: Weight Reduction Case Study of a Premium Road Bicycle Crank Arm Set by Implementing Beralcast® 310, Vancouver (2013)

http://www.springer.com/978-3-319-66865-9

Industrializing Additive Manufacturing - Proceedings of Additive Manufacturing in Products and Applications - AMPA2017

Meboldt, M.; Klahn, C. (Eds.)
2018, XII, 362 p. 226 illus., Hardcover
ISBN: 978-3-319-66865-9